THE USE OF TERRASAR-X TIME-SERIES FOR MONITORING THE HYDRIC STATES OF SLAKING CRUSTS IN AGRICULTURAL FIELDS

Maëlle Aubert[1*], Nicolas Baghdadi[2], Mehrez Zribi[3], Mahmoud El Hajj[4]
[1]Phd Student, CNES - Noveltis, UMR TETIS, 500 rue jean françois breton, Montpellier 34093, France;
Email: maelle.aubert@teledetection.fr

[2] CEMAGREF, UMR TETIS, 500 rue jean françois breton, Montpellier 34093, France;
E-mail: nicolas.baghdadi@teledetection.fr

[3]IRD-CESBIO, 31401 Toulouse, France; E-mail: mehrez.zribi@ird.fr

[4] NOVELTIS, 31520 Ramonville-Saint Agne, France ; E-mail: mahmoud.elhajj@noveltis.fr

KEY WORDS: TerraSAR-X, slaking crust, soil moisture, time-series, bare soil.

ABSTRACT: Through the modification of water-retention properties and infiltration rates, slaking crust structures cause significant environmental problems such as runoff and sheet erosion on agricultural surfaces. Moreover, the state of soil surface structure is one of the most important factors considered in erosion risk assessment. In this paper, we assess the potential of TerraSAR-X time series acquired at very high spatial resolution (1m) to detect the spatial distribution of slaking crust at the within plots scale, and to monitor the dynamics of slaking crust hydric states. We analyzed the behavior of the TerraSAR-X signal for two configurations HH-25° and HH-50°, with regard to several soil moisture content and slaking crust conditions that were recorded during field campaigns in the winter of 2009 and 2010 on the Orgeval watershed (France).
For both TerraSAR-X configurations no direct link between the soil crust and the backscattered signal was observed. Nevertheless, TerraSAR-X signal variations within plots were found to be correlated to the hydric evolution of the soil crust. In fact, soil moisture may differ between two soil structures, resulting in variations in the TerraSAR-X signal. All within plot difference of soil moisture greater than 3% could be detected and tracked. Furthermore it is possible to track surface degradation due to the slaking process using time-series of TerraSAR-X data. Thus, the dynamics of slaking crust hydric states within plots can be monitored using TerraSAR-X data.

1. INTRODUCTION

Soil structure plays a crucial role in the distribution of precipitation between surface runoff and infiltration. The knowledge of soil structure state is of considerable importance in various applications, such as hydrology, risk prediction, and agriculture (Le Bissonnais et al., 1998; Auzet et al., 1995). Slaking crust (the disintegration of ploughed clods) is a physical degradation of soil surface structure resulting from the rainfall impact on the topsoil. This phenomenon is commonly observed on loamy soils and the susceptibility of topsoil for slaking depends mainly on its material properties such as soil composition, organic matter content and content of carbonates. Soils covered by this thin crust layer have a low permeability. Thus surface covered by slaking crust have a low infiltrability which promotes runoff (Augeard, 2006; Musy and Soutter, 1991). The presence of slaking crust on bare field causes significant environmental problems. On agricultural watershed, erosion rate and flood genesis increase with the increase of the area covered by slaking crust (Assouline, 2004). Also, spatial extent and the hydric state of slaking crust must be taking into account for constraining the initial conditions of infiltration/runoff rates when modeling overland flow and erosion at the watershed scale. Improve the understanding of the temporal and spatial dynamics of slaking crust in agricultural watershed is essential to prevent such risks at regional scale.
In this respect, remote sensing technique offered a unique opportunity to characterize soil surface in large areas of land in a short time. More specially, Synthetic-aperture radar (SAR) sensor offers a powerful tool to provide accurate and repetitive spatial data under any weather conditions, both day and night (Dobson & Ulaby, 1986; Fung, 1994; Hallikainen et al., 1985; Ulaby et al., 1986).
Many studies have already demonstrated that soil roughness and moisture can be retrieved from SAR data acquire over bare soil surface. The sensitivity of SAR signal to these soil surface characteristic depends on various radar parameters such as polarization, incidence angle and frequency. Few studies have examined the effects of soil slaking on microwave remote sensing sensors. In X-band, Stolp & Janse (1986) have carried out a multiple linear regression to relate the backscattering coefficient (HH-15°) to the degree of slaking, the direction of tillage and the incidence angle. Their results are promising and provide good estimates of the degree of slaking (with accuracy between 56% and 78%). The new TerraSAR-X sensors operating in X-band with only one polarization can provide data very sensitive

to soil moisture whatever the incidence angle (0.411 dB/% HH-25°; 0.323 dB/% HH-50°) (Aubert et al., 2011). With this sensor, very low variations of soil moisture (<5%) can be detected within bare agricultural fields (Paris Anguela et al., 2010). As areas covered by slaking crust have a lower infiltration rates than soil without crust, a soil moisture difference between the two soils may be created. Consequently, the presence or absence of slaking crust on the topsoil layer may induce dielectric contrasts on the backscattered TerraSAR-X signal. Therefore TerraSAR-X sensor should provide valuable information for managing the degradation of soil surface structure because data could both permit to identify soil crusts spatial extent and to determine the hydric state.
In the first part of this paper, we assess the potential of X-band SAR data acquired by TerraSAR-X sensor to detect the spatial distribution of slaking crust at plots scale. In a second part, TerraSAR-X data time series are used to monitor the dynamics of slaking crust hydric states.

2. MATERIAL AND METHODS

2.1 Study site

The study site is the Orgeval watershed (104 km²), located to the east of Paris in France (Latitude: 48°51'; longitude 3°07'E; Figure 1). The main land use is arable farming intended for growing wheat and maize. It is flat and the topsoil composition is predominantly loamy (17% clay, 78% silt, and 5% sand). This soil composition promotes crust development, which increases soil sealing and causes runoff (Boiffin et al., 1990; Eimberck, 1990). The Orgeval watershed has been managed since 1962 as an experimental basin for hydrological research by the Agricultural and Environmental Engineering Research Center (CEMAGREF) research institute.

Figure 1. Location of the Orgeval watershed (central coordinates: 48°52'N, 3°06'E).

2.2 TerraSAR-X Data

Eleven TerraSAR-X images were used in this study. They are acquired in spotlight mode (pixel spacing ~1m) between March 2009 and March 2010. Images were obtained with incidence angles of 25° and 50°, and at HH polarizations (Table 1).

SAR acquisition date dd/mm/yy	Polarization	Incidence angle	In situ soil moisture (%) [Min; Max]
17/03/09	HH	25°	[24.7; 32.3]
18/03/09	HH	50°	[24.5; 29.8]
25/03/09	HH	50°	[24.1; 31.0]
26/03/09	HH	25°	[23.9; 32.7]
08/04/09	HH	25°	[16.8; 27.5]
09/04/09	HH	50°	[15.2; 26.3]
01/03/10	HH	50°	[33.4; 39.8]
02/03/10	HH	25°	[32.7; 39.0]
04/03/10	HH	25°	[27.3; 34.3]
12/03/10	HH	50°	[12.6; 29.0]
13/03/10	HH	25°	[14.9; 26.3]

Table 1. Characteristics of TerraSAR-X images and in situ soil-moisture measurements.

First, SAR data were radiometrically calibrated, using the following equation (Eineder, 2011):

$$\sigma^{o}_{i\,dB} = 10 \cdot \log_{10} (Ks \cdot DN_i^2 - NEBN) + 10 \cdot \log_{10} \sin(\theta_i) \quad (1)$$

This calibration permits to convert the digital numbers of each pixel (DN_i) into a backscattering coefficients (σ°_i) corrected for sensor noise (NEBN) on decibels scale. This calibration process takes into account the radar incidence angle (θ) and the calibration constant (Ks) provided in the image data.

Images were then co-registered using aerial orthophotos (50-cm spatial resolution) with a root mean square error of the control points of approximately one pixel (i.e. 1 m). This co-registration error was overcome by removing the boundary pixels (two pixels wide) from each training plot relative to the limits defined by the GPS control points. All these calibration processes makes it possible to carry out multi-temporal analysis of different images.
In this study only radar signal from bare soil were used. Also, selected areas are identified and the mean signal calculated was used as the radar signature of each selected part of field. This database permits to well understand the limit of soil crust observations with TerraSAR-X sensor because it illustrates three cases of soil structure for each configuration (HH-25°, HH-50°): without slaking crust (April, 2009), with slaking crust observable on TerraSAR-X data (March 17 and 18, 2009; March 12 and 13, 2010), and with slaking crust unobservable on TerraSAR-X data (March 25 and 26, 2009, March 1 and 2; 2010).

2.3 Experimental measurements

Simultaneously to TerraSAR-X acquisitions, ground measurements were performed in seven bare training plots in 2009 and six in 2010 (± three hours around the satellite overpass time) (Figure 2). All training plots were flat (slope < 1%) and don't have marked row directions because they correspond to old winter ploughed without row direction (isotropic surface).
The percentages of clay, sand and silt contents were determined using soil samples collected within each training plot. Results showed that the surface soils within the training plots could be classified into two categories of loam: Soil I: clay = 24% ± 1.9%; silt = 71% ±1.7%; sand = 5% ± 1.5%; Soil II: clay = 16% ± 0.9%; silt = 78% ± 2%; sand = 6% ± 1.3%. The major differences between these two soils correspond to small variations in clay and silt contents (clay = 8%, silt = 7%). The largest difference in clay content between soil I and soil II was found in plot D (~10%), and the smallest value was found in plot G (~3%). The differences in sand content were very small (mean ~1%).

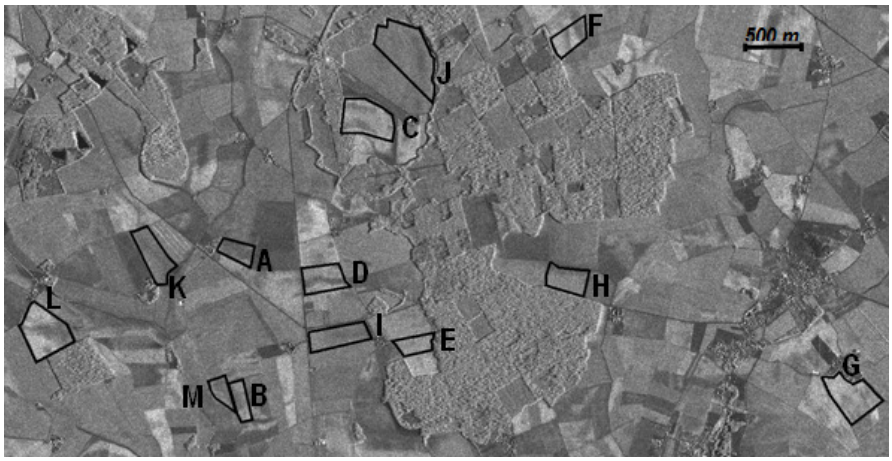

Figure 2. Subset of a TerraSAR-X image (17 March 2009) acquired over the Orgeval watershed. Plot A to G are the training plots investigated in 2009 field survey, plots H to M are those of 2010.

Differences of grain size distribution (silt, clay), organic matter, and carbonate content (not analyzed here) between soil II and soil I generate difference of soil structure. Also, a slaking crust phenomenon is commonly observed on the Soil II. The presence or absence of slaking crust on the soil surface was noted by pedologist expert during the 2009 and 2010 field survey. This degraded structure is visible to the naked eye because slaking crust blocks the porosity of the soil surface and creating a layer of compacted soil. The stagnation of water and the presence of a thin, continuous and consistent surface layer (crust) indicate the spatial extent of the slaking crust. For each acquisition date of March 2009 and 2010, a slaking crust with a thickness of approximately 1 cm is observed on the more loamy part of our training plot (soil II). In April 2009, no slaking crusts were observed within the training plots due to tillage operations that had removed the soil crusts and increased the porosity of the topsoil.
No experimental measurements of crust hydric properties were conducted (infiltration capacity) but gravimetric soil moisture samples (depth: 0-5 cm) were collected on the crusted part of our training plot (soil II) and on the without crust part of tour training plot (soil I). All gravimetric measurements were converted into volumetric moisture (*mv*) based on bulk density, and the location of each gravimetric measurement was recorded using a GPS device. Thus, soil moisture of each part of a plot was assumed to be equal to the mean value estimated from the samples collected in each part. The two field surveys in 2009 and 2010 covered a large range of soil moisture, between 12.6% and 39.8% (Table 1). Finally, meteorological data (precipitation and temperature) were also obtained from five meteorological stations installed in the basin. Figure 3 shows the mean values of meteorological data recorded in 2009 and 2010 at the five stations.

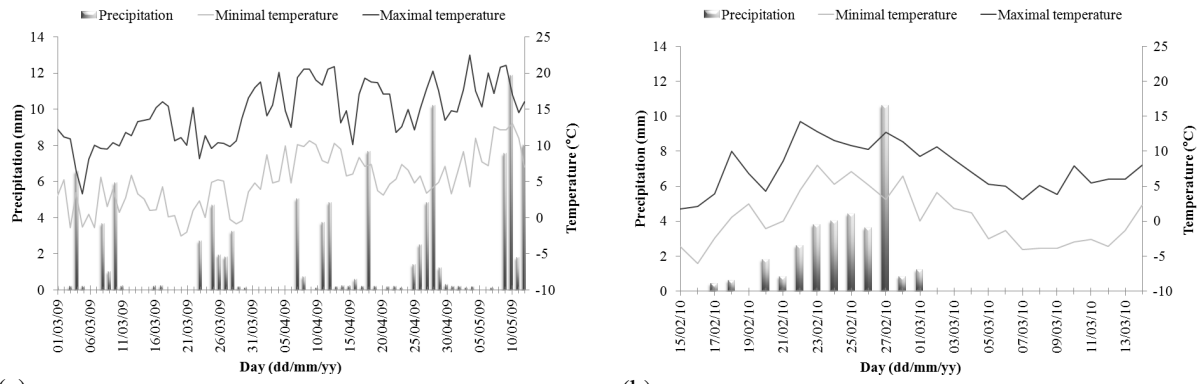

Figure 3. Daily precipitation (mm), minimum and maximum temperatures averaged over the five stations installed in the basin in 2009 (a) and 2010 (b).

3. RESULTS

Heterogeneities within plots were observed in some TerraSAR-X images on March 17 and 18, 2009 (Figures 2 and 4). These variations within the training plots were also observed in the end of the TerraSAR-X time-serie acquired on 2010 (March 12 and 13; Figure 4). The variations in the TerraSAR-X signal within plots were spatially correlated with the variations in soil structure observed in situ. In fact, according to the soil structure observation, the zones with low radar-signal values (darker zones) on March 17 and 18, 2009 (Figures 4a and 4b) were no crusted (soil I: 24% clay, 71% silt and 5% sand) and the zones with high radar-signal values correspond to slaking crust structure (brightest zones; soil II: 16% clay, 78% silt and 6% sand). On the time-series of 2010, the part of training plot crusted also appears brighter than the part of training plot without crust (March 12 and 13; Figures 4j and 5k).

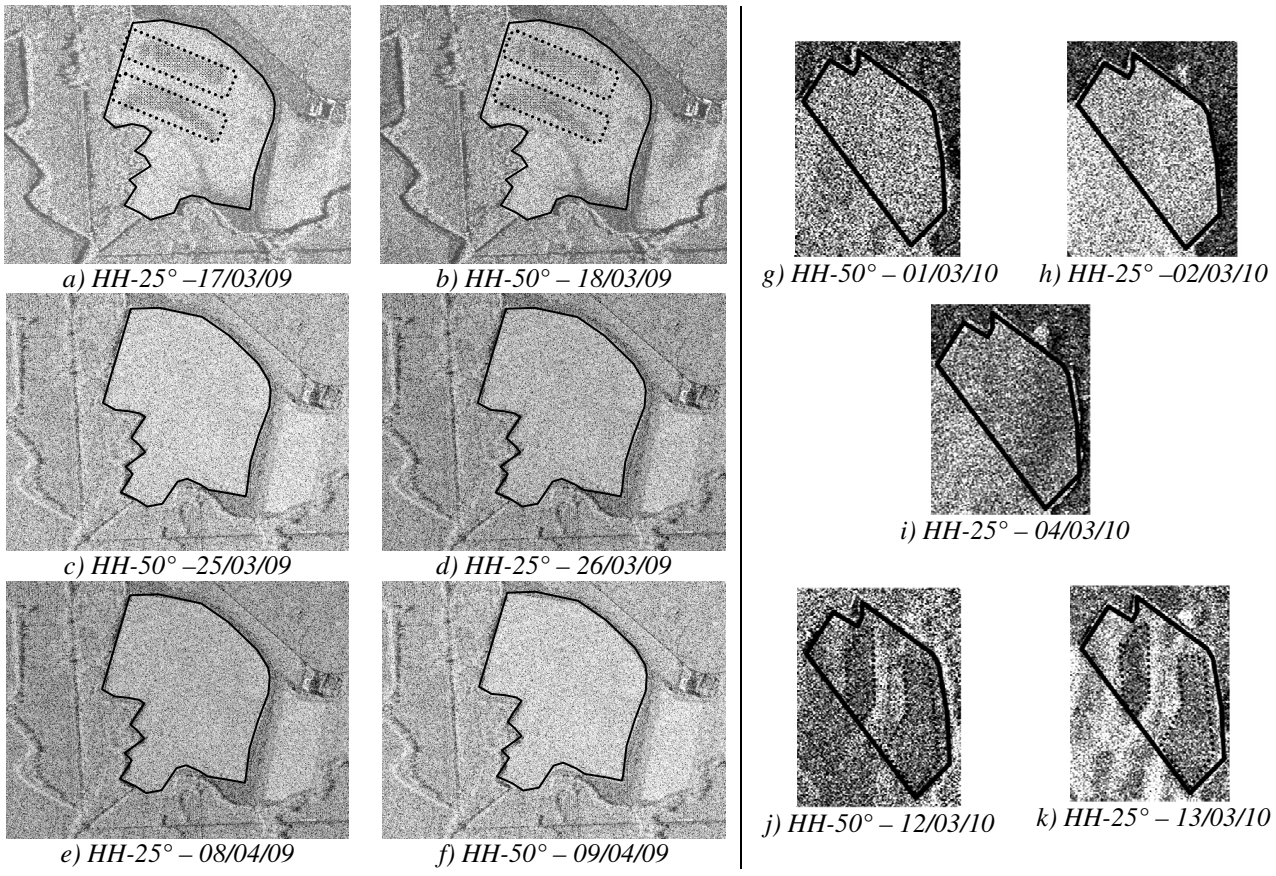

Figure 4. Variations in TerraSAR-X signal within the two training plots (outlined in black) C (2009 acquisitions: a to f) and J (2010 acquisitions: g to k). Soil I is outlined with a dotted black line (darker zone), and soil II corresponds to the brighter zones.

The spatial correlation between TerraSAR signal variations and slaking crust extent within bare fields could be due to

three factors: soil moisture, surface roughness or soil composition. At X-band, the variation of soil composition between soil crusted and not crusted is negligible, and the surface roughness within plot will be supposed constant or with little difference (causing low variation in the backscattering coefficient) (Aubert et al., 2011). So, variation in the backscattering coefficient at within plot scale was linked to a soil moisture variation, and detecting spatial distribution of slaking crust is only possible in the case of soil moisture variations between crusted and no crusted soils.
The differences in soil moisture between soil II and soil I ($mv_{soil\ II}$ - $mv_{soil\ I}$) were compared to the differences in the TerraSAR signal ($\sigma°_{soil\ II}$ - $\sigma°_{soil\ I}$) for HH-25° and HH-50°, with regard to several conditions of soil structure that were recorded during field campaigns in the winter of 2009 and 2010 (Figure 5). Figure 5 showed that whatever the TerraSAR-X configuration (HH-25°, HH-50°), the mean difference in signal between soil II and soil I increased with the difference of soil moisture measured in situ.
Thus, according to the sensitivity of TerraSAR-X to soil moisture (25°: 0.411 dB/%; 50°: 0.323 dB/%), it is possible to track slaking crust extent once the difference in soil moisture content between soils crusted and not crusted is greater than 2.4% at low incidence angle and 3.1% at high incidence angle.

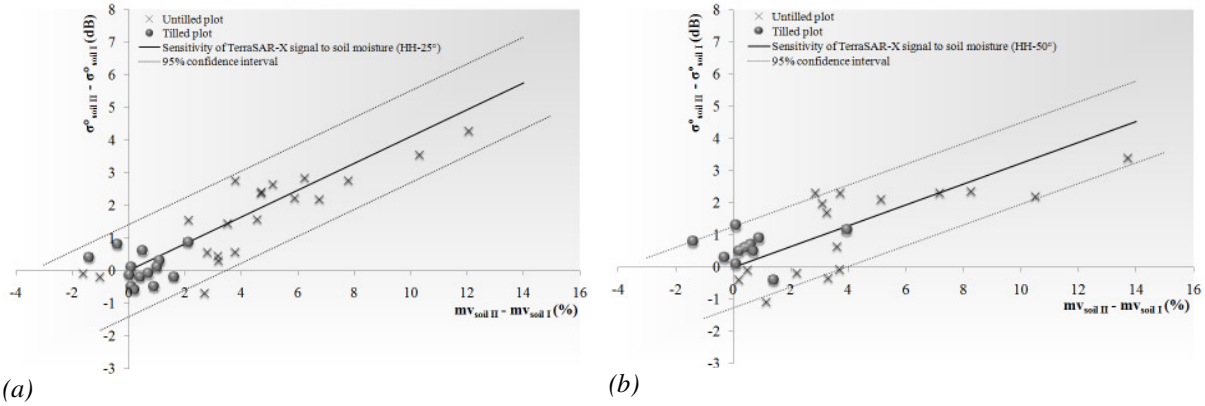

(a) *(b)*

Figure 5. Difference between the TerraSAR-X signal of soil II and that of soil I (dB) in function of the difference of soil moisture measured in situ (%) for HH-25°(a) and HH-50°(b).. Cross and round correspond respectively to tilled and untilled training plot (with crust). The black line correspond to the sensitivity of TerraSAR-X signal to soil moisture, the dote line correspond to the confidence interval at 95%.

In the following, we used the TerraSAR-X 2009 and 2010 times series to monitor the hydric process which occurred within training plot with present a slaking crust. To do this, the difference of backscattered signal between soil crusted (soil II) and not crusted (soil I) was used, and compared to meteorological data and in situ soil moisture measurements.
At the beginning of the TerraSAR-X time serie acquired in 2009, the mean difference in signal calculated from March 17 (25°) and March 18 (50°) between the soil II and soil I zones was respectively of +2.2 dB and +2.5 dB for a mean difference in moisture content of +4.7% and 4.5%. Indeed, during the winter dry period (March 11 to March 22, Figure 3a), soil I dries faster than soil II. In soil II, evaporation is limited by the crust, and the moisture content is retained longer than in soil I. Thus, the moisture-content values of soil I were lower than those of soil II.
On March 25 and 26, the mean difference in signal between soil II and soil I zones was less than 1 dB and the average difference in moisture content was less than 1%. Thus, no variation in either soil moisture or TerraSAR-X signal was observed within the plots on these dates. After rainy events (2.7 mm on March 23 and 4.7 mm only three hours before the March 25 acquisition; Figure 3a), the moisture content of soil I increased strongly (by approximately +4.5%) because soil I absorbed both precipitation and streaming water coming from soil II. The moisture content of soil II increased slightly (by approximately 1%) because the soil crust prevented water infiltration and favored hydric inertia. On March 17 and 18, soil II had greater moisture content than soil I. As the moisture content of soil I increased and the moisture content of soil II stayed constant, the difference in moisture content between the two soils disappeared. For the other acquisition dates between April 8 and May 11, 2009, tillage had destroyed the soil crust and increased the porosity of soil II. Without crust, the compositions of the two soils were too similar to generate a difference in moisture content between soil I and soil II (< 1%), and no differences in signal were observed between the two soils.
The 2010TerraSAR-X time serie, showed the difference of hydric process between soil crusted and not crusted under a winter dry period (March 1 to 13, 2010; Figure 3b). On March 1 and 2, the mean difference in signal between soil II and soil I zones was less than 1 dB and the average difference in moisture content was less than 3%. Then, according to meteorological data (Figure 3b), the moisture content decreased strongly on soil I and slightly on soil II because the soil crust prevented water evaporation and favored hydric inertia. Consequently, on March 12, and 13 the mean difference in signal between the soil II and soil I zones was respectively of +1.7 dB and +2.2 dB for a mean difference in moisture content of approximately +6%.

Thus, variations in the TerraSAR-X signal within plots are correlated with differences in the soil surface structure between the two soils. The slaking crust on soil II generated differences in moisture content between soil I and soil II under certain meteorological conditions.

4. CONCLUSION

This study analyzes the potential of high-spatial-resolution data from the TerraSAR-X sensor to identify and monitor the slaking crust of bare agricultural soils at within-plot scales. The backscattering coefficients obtained from multi-temporal SAR acquisitions at HH polarization and two incidence angles (25° and 50°) were compared to ground observations and measurements. Our results are promising for retrieving slaking crust extent from TerraSAR-X data and for monitoring the dynamics of slaking crust hydric states within plots. The slaking crust extent detection is only dependent on the conditions of acquisition (difference of hydric state between soil crusted and not crusted) and can be carried out with either low or high incidence angle. This slaking crust extent map could be a relevant parameter in erosion and flood modeling. The monitoring of slaking crust hydrics state also could reduce uncertainties in water budgets and thus improve the predictive capabilities of erosion and flood model. In further work, an assimilation of slaking crust soil moisture data estimated from TerraSAR images could be used as an input data to improve the forecast models.

Acknowledgments
The authors wish to thank the CNES (French Space Agency) and the company Noveltis (scientific engineering studies) which finance the PhD thesis of Maelle Aubert. We extend our thanks to DLR (the German Space Agency) for kindly providing the TerraSAR-X images (proposal HYD0007 and HYD0542). We also thank Cemagref (Antony) staff for helping to collect field data.

5. REFERENCES

Aubert M., Baghdadi N., Zribi M., Douaoui A., Loumagne C., Baup F., El Hajj M., and Garrigues S., 2011. Analysis of TerraSAR-X data sensitivity to bare soil moisture, roughness, composition and soil crust», Remote Sensing of Environment 115: 1801–1810.
Assouline, S., 2004. Rainfall-induced soil surface sealing: a critical review of observations, conceptual models, and solutions. Vadose Zone Journal., 3: 570-591.
Augeard, B. 2006. Mécanismes de genèse du ruissellement sur sol agricole drainé sensible à la battance. Etudes expérimentales et modélisation. Doctorat Sciences de l'eau, Unité de Recherche Hydrosystèmes et Bioprocédés, ENGREF 06ENGR0010, 236 p.
Auzet, A.V., Kirkby, M.J., Van Dijk, P. 2005. Surface characterisation for soil erosion forecasting. Catena, vol. 62, n° 2–3: 77–78.
Dobson, M.C., & Ulaby, F.T. 1986. Active microwave soil moisture research. IEEE Transactions on Geoscience and Remote Sensing, vol. GE-24, n° 1: 23-36.
Fung, A,K. 1994. Microwave Scattering and Emission Models and their Applications. Artech House, Norwood, Massachussetts : 573 p.
Le Bissonnais, Y., & Singer, M.J. 1992. Crusting, Runoff and erosion Response to soil Water Content and Successive Rainfalls. Soil Science Society American Journal, vol. 56: 1898-1903.
Musy, A., et Soutter, M. 1991. Physique du sol. Presses Polytechniques et Universitaires Romandes, Lausanne, Suisse, 335p.
Paris Anguela, T., Zribi, M., Baghdadi, N., Loumagne, C. 2010. Analysis of local variation of soil surface parameters with TerraSAR-X radar data over bare agricultural fields. IEEE Transactions on Geoscience and Remote Sensing vol. 48, n° 2: 874–881.
Stolp, J., Janse, A.R.P. 1986. X-band radar backscattering for detecting spatial distribution of soil slaking. ITC Journal, vol. 1: 82-87.
Ulaby, F.T., Moore, R.K., & Fung, A.K. 1986. Microwave Remote Sensing, Active and Passive, From Theory to Applications, vol. 3, Artech House, Inc., 685 Canton Street, Norwood, MA 02062, 1098 p.